Reprinted from LANGMUIR, 1995, *11*.

Scanning Force Microscopies Can Image Patterned Self-Assembled Monolayers

James L. Wilbur, Hans A. Biebuyck, John C. MacDonald, and George M. Whitesides*

Department of Chemistry, Harvard University, Cambridge, Massachusetts 02138

Received July 14, 1994. In Final Form: September 26, 1994[⊗]

This paper demonstrates that scanning probe microscopies (SPMs) can image patterned self-assembled monolayers (SAMs) formed by microcontact printing. Lateral force microscopy (LFM) and force modulation microscopy (FMM) showed contrast between regions of patterned SAMs terminated by different chemical functionalities. Normal force microscopy (NFM) typically showed less contrast than LFM or FMM but provided information about the topography of the surface. Chemical functionality (at the interface between the SAM and air) dominated imaging in these experiments. Changes in the morphology of the surface or changes in the humidity of the environment for imaging did not influence significantly the contrast in our experiments. The sharpness of the contrast suggests the use of LFM and SAMs in studying tribology on the submicrometer scale.

Introduction

This paper explores the use of scanning force microscopies[1] (SFMs) to image patterned self-assembled monolayers (SAMs) formed by microcontact printing[2,3] (μCP) of functionalized alkanethiols, $HS(CH_2)_nY$, on gold. Imaging these patterned SAMs requires sensitivity to the chemical composition of a surface since only small differences in the molecular structure of the constituent alkanethiolates distinguish regions of the patterned SAM. A number of techniques have been used to image patterned SAMs: among the most useful are XPS,[4] condensation figures,[5,6] SEM,[7] Auger spectroscopy,[8-10] and SIMS.[9,11] Lateral force microscopy (LFM) is sensitive to changes in the chemical composition of a surface,[12,13] has magnification ($>10^7$) similar to STM, and, in conjunction with normal force microscopy (NFM), provides topographical information. Here we demonstrate that it can provide excellent imaging of patterned SAMs. LFM imaging of patterned SAMs also has the potential to provide the basis for a new approach to experimental tribology, with observation localized on regions less than 100 nm in width.

LFM works on a principle similar to other AFM methods by measuring the interactions between a probe and the features on the surface of a substrate (Figure 1). A cantilever (force constant ~1 N/m) supports a silicon nitride tip (radius of curvature ~1000 Å) placed in contact with a substrate. A three-axis piezoelectric scanner rasters the sample beneath the cantilever and tip. The top of the cantilever reflects a laser beam onto a four-quadrant photodetector: topographical variations in the surface deflect the cantilever and change the position of the laser beam on this photodetector. A feedback loop uses the difference between signals from the upper and lower halves of the photodetector to adjust the z-piezoelectric ceramic and maintain constant force between the tip and sample. The voltage required to adjust the z-piezoelectric ceramic generates the NFM data. Higher voltage corresponds to features with relatively greater height, represented by bright pixels in the NFM image. Twisting of the cantilever, due to changes in the interactions between the tip and surface, also changes the position of the laser beam on the photodetector. A difference between signals from the left and right sides of the photodetector is interpreted as a lateral force. A relatively larger positive difference between the left and right sides of the photodetector corresponds to greater lateral force, represented in the LFM image by brighter pixels. Simultaneous detection of all quadrants of the photodetector gives both LFM and NFM data (at constant force) in the same scan.

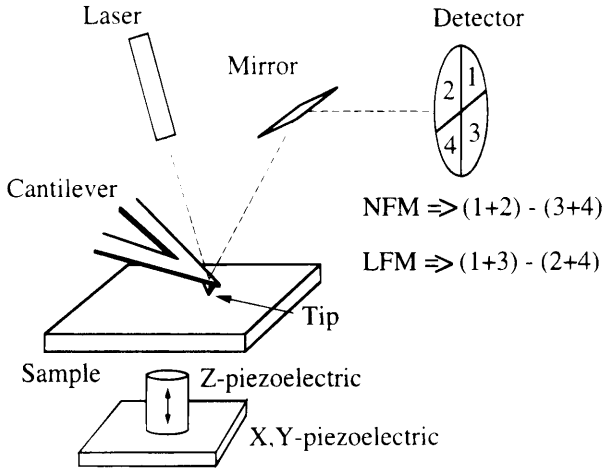

Figure 1. Schematic of the detection system for scanning probe microscope. See text for details.

Patterned SAMs formed by μCP have many applications, including microfabrication,[2,3] studies of wetting and nucleation phenomena,[6,14,15] protein[16] and cellular adhe-

* Author to whom correspondence should be addressed.

[⊗] Abstract published in *Advance ACS Abstracts*, February 15, 1995.

(1) For recent reviews of scanning probe microscopy studies on organic surfaces, see Fuchs, H. *J. Mol. Struct.* **1993**, *292*, 29. Frommer, J. *Angew. Chem., Int. Ed. Engl.* **1992**, *31*, 1265.

(2) Kumar, A.; Whitesides, G. M. *Appl. Phys. Lett.* **1993**, *63*, 2002–2004.

(3) Kumar, A.; Biebuyck, H. A.; Whitesides, G. M. *Langmuir* **1994**, *10*, 1498–1511.

(4) López, G. P.; Biebuyck, H. A.; Harter, R.; Kumar, A.; Whitesides, G. M. *J. Am. Chem. Soc.* **1993**, *115*, 10774–10781.

(5) López, G. P.; Biebuyck, H. A.; Frisbie, C. D.; Whitesides, G. M. *Science* **1993**, *260*, 647–649.

(6) Kumar, A.; Whitesides, G. M. *Science* **1994**, *263*, 60–62.

(7) López, G. P.; Biebuyck, H. A.; Whitesides, G. M. *Langmuir* **1993**, *9*, 1513–1516.

(8) Stenger, D. A.; Georger, J. H.; Dulcey, C. S.; Hickman, J. J.; Rudolph, A. S.; Nielsen, T. B.; McCort, S. M.; Calvert, J. M. *J. Am. Chem. Soc.* **1992**, *114*, 8435–8442.

(9) Frisbie, C. D.; Martin, J. R.; Duff, R. R. J.; Wrighton, M. S. *J. Am. Chem. Soc.* **1992**, *114*, 7142–7145.

(10) Hickman, J. J.; Ofer, D.; Zou, C.; Wrighton, M. S.; Laibinis, P. E.; Whitesides, G. M. *J. Am. Chem. Soc.* **1991**, *113*, 1128–1132.

(11) Tarlov, M. J.; Newman, J. G. *Langmuir* **1992**, *8*, 1398–1405.

(12) Overney, R. M.; Meyer, E.; Frommer, J.; Brodbeck, D.; Luthi, R.; Howald, L.; Guntherodt, H.-J.; Fujihira, M.; Takano, H.; Gotoh, Y. *Nature* **1992**, *359*, 133–135.

(13) Frisbie, C. D.; Rozsnyai, L. F.; Noy, A.; Wrighton, M. S.; Lieber, C. M. *Science* **1994**, *265*, 2071–2074.

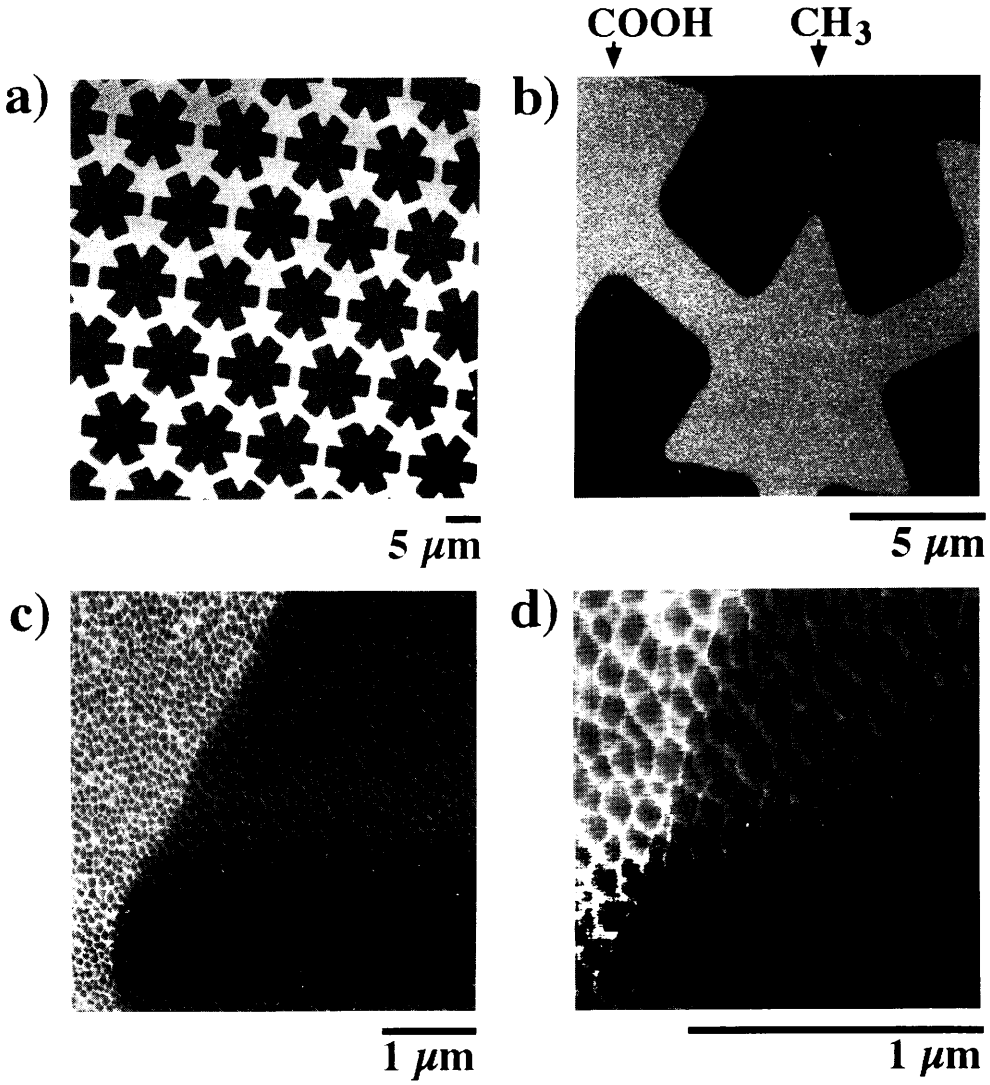

Figure 2. Lateral force microscopy reveals contrast between adjacent regions of SAMs with terminal CH_3 groups (dark, lower torsion) or terminal COOH groups (light, higher torsion). Microcontact printing of hexadecanethiol on gold (1000 Å thick) formed the initial pattern; exposure of this sample to an ethanolic solution of mercaptohexadecanoic acid (~5 mM) completed the SAM in regions where the gold surface was not derivatized by hexadecanethiol. Texture in these images reflected the distribution of crystallites on 1000 Å gold evident in NFM images acquired simultaneously. Data for all of these images were collected as the tip moved from left to right.

sion,[17] and the patterned formation of microcrystals and microcrystal arrays.[3] In this paper we explore some of the parameters associated with imaging these patterned SAMs by LFM.

Results and Discussion

LFM images regions of different chemical functionality in patterned SAMs. In initial studies, we patterned gold by μCP to form regions of SAMs terminated by CH_3 (γ_{sv} = 18 ergs cm^{-2})[18] or COOH (γ_{sv} > 100 ergs cm^{-2}).[19] These two functional groups were chosen since they spanned the range of surface polarities and free energies conveniently available with organic surfaces. Previous studies[3,7,15] showed that μCP produced homogeneous (>99% pure) regions of different chemical functionality separated by sharp boundaries (<100 nm). LFM showed contrast between regions terminated by CH_3 and COOH and reproduced the pattern caused by microcontact printing (Figure 2). The contrast evident between CH_3 and COOH arose from differences in the interactions between the cantilevered tip and the surface in each region: the tip experienced lower torsion in regions of the patterned SAM terminated by CH_3 than in regions terminated by COOH. Changes in torsion on the cantilever in LFM experiments have been interpreted generally as changes in friction between the tip and surface.[12,20,21] Plausible factors that influence the torsion between the tip and surface are (i) the interfacial free energy between the tip and the surface, (ii) adsorbates between the tip and the surface and modifications of interactions between the tip and surface due to these adsorbates (for example, capillary forces due to condensed water bridging the tip and the surface), and (iii) the morphology of the sample (see below).

(14) Biebuyck, H. A.; Whitesides, G. M. *Langmuir* **1994**, *10*, 4581–4587.
(15) Biebuyck, H. A.; Whitesides, G. M. *Langmuir* **1994**, *10*, 2790–2793.
(16) Prime, K. L.; Whitesides, G. M. *Science* **1991**, *252*, 1164–1167.
(17) Singhvi, R.; Kumar, A.; Lopez, G. P.; Stephanopoulos, G. N.; Wang, D. I. C.; Whitesides, G. M.; Ingber, D. E. *Science* **1994**, *264*, 696–698.
(18) Chaudhury, M. K.; Whitesides, G. M. *Langmuir* **1991**, *7*, 1013–1025.
(19) γ_{sv} for SAMs on gold terminated by carboxylic acids is sensitive to the state of ionization of these groups. The contact angle of water at pH = 1 on these surfaces (<10°), where the carboxylic acids remain largely protonated, provides the lower limit for γ_{sv}. See: Lee, R. T.; Carey, R. I.; Biebuyck, H. A.; Whitesides, G. M. *Langmuir* **1994**, *10*, 741–749.
(20) Meyer, E.; Overney, R. M.; Brodbeck, D.; Howald, L.; Luthi, R.; Frommer, J.; Guntherodt, H.-J. *Phys. Rev. Lett.* **1992**, *69*, 1777–1778.
(21) Overney, R. M.; Meyer, E.; Frommer, J.; Guntherodt, H.-J. *Langmuir* **1994**, *10*, 1281–1286.

Boundaries between gold crystallites, which were local regions of high curvature, appeared in the LFM image as changes in the intensity at a length similar to the size and distribution of these crystallites as characterized topographically by NFM. These changes in the curvature of the surface necessarily appeared in the LFM images.[22] Variations in the slope of the surface (going up or down a crystallite, for example) cause the cantilever to bend (or twist) and change the position of the light on the photodetector: changes in the difference between signals from the left and right sides of the photodetector result in contrast in the LFM image.

The direction of scanning affected the contrast observed by LFM. Data for the images in Figure 2 were collected with the tip scanning from left to right. As the tip moved up a crystallite (scanning from left to right), a positive difference between signals from the left and right sides of the photodetector (brighter in Figure 2) registered. Going down a crystallite caused the difference in photocurrent to become (relatively) more negative (darker in Figure 2). Two observations support these conclusions: (i) the contrast between crystallites is generally brightest where the edge of the crystallite runs perpendicular to the scanning direction (Figure 2d); (ii) the left sides of the crystallites (going up while scanning left to right) are uniformly brighter than the right sides of the crystallites (particularly evident in the CH_3 terminated region in Figure 2d). Reversing the direction of scanning inverted the contrast for the entire image. This observation was expected since changing the direction of scanning is equivalent to changing the sign of the difference signal between the left and right sides of the photodetector.

An additional component to the contrast between crystallites in Figure 2 may result from changes in the area of contact between the tip and surface due to changes in the curvature of the surface. We did not test this possibility. The greater differential force measured by LFM in regions between crystallites, where curvature of the gold surface is higher than on top of crystallites, may also reflect higher capillary effects on the AFM tip due to adsorbate films. We consider contributions of films of water and surface roughness to imaging by LFM in the proceeding sections.

LFM imaging of patterned SAMs has several strengths. LFM has high resolution and is sensitive to topographic features of the surface: LFM showed that the border (due to μCP) between regions terminated by CH_3 and COOH was sharp (<50 nm) and followed the depressions (2–3 nm) between crystallites (Figure 2d). LFM also appeared to be nondestructive (compared to SEM,[7] for example) during imaging. Repeated scanning of the tip across the surface did not significantly alter the contrast between regions terminated by CH_3 or COOH: imaging repeatedly the same region (of a patterned SAM) produced essentially identical images. This result demonstrated that imaging by LFM, under the conditions used in this study, was nondestructive.

Imaging patterned SAMs by NFM typically (>95% of samples studied) showed less contrast between regions terminated by CH_3 or COOH than did imaging by LFM.[23] Under conditions used for LFM, NFM imaging of a patterned SAM (formed by μCP) showed only faint contrast between regions terminated by CH_3 and COOH. (Figure 3a). NFM detected less than 0.5 nm difference in height (limited by noise) between regions terminated by CH_3 and COOH. Imaging this same sample by LFM showed strong contrast between regions terminated by CH_3 or COOH (Figure 3a, inset). Imaging by NFM provided topographical information: NFM revealed (Figure 3) the characteristic roughness of a 1000 Å thick gold surface[24] (prepared by electron-beam evaporation). Occasionally (<5% of samples), the contrast observed by NFM between regions of a patterned SAM terminated by CH_3 (dark) and COOH (light) was comparable to the

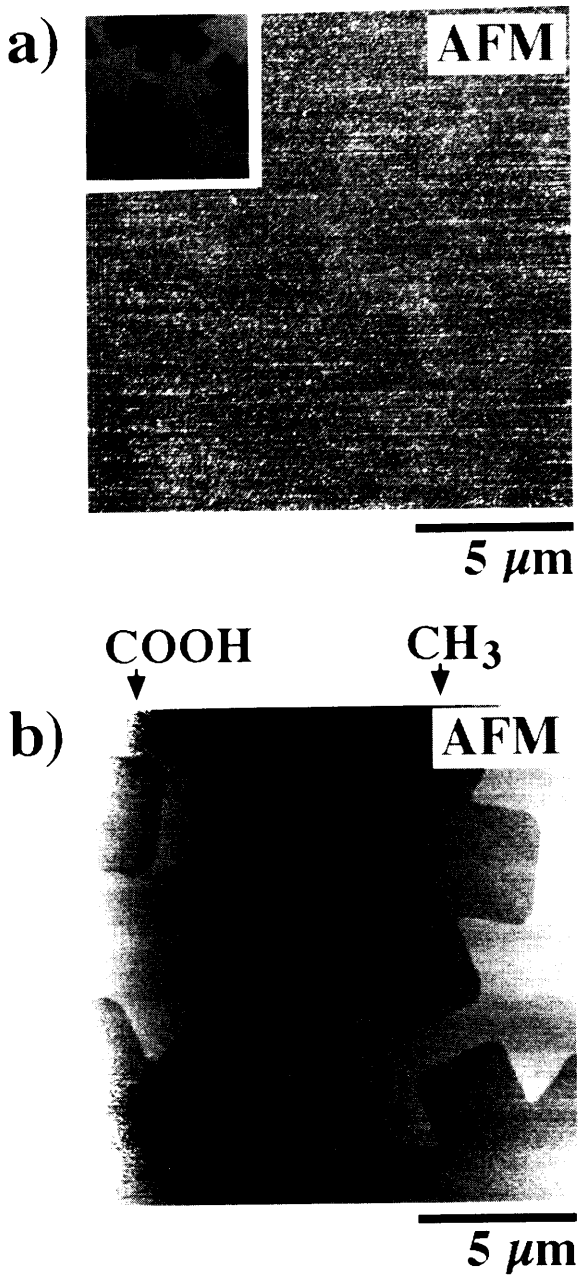

Figure 3. (a) Typically, attempts to image patterned SAMs by NFM showed little (or no) contrast between regions terminated by CH_3 or COOH. The very faint contrast (between regions terminated by CH_3 and COOH) in (a) corresponds to the pattern observed when imaging the same sample by LFM (inset, a). NFM revealed the topography of the gold surface: the texture in (a) corresponds to crystallites on 1000 Å thick gold. (b) Occasionally (<5% of samples), imaging a patterned SAM by NFM showed contrast between SAMs terminated by CH_3 (dark) or COOH (light). The increased contrast in these samples is due probably to increased adsorbates on the (more hydrophilic) COOH regions. In (b), regions of the sample terminated by COOH were ~2 nm higher than regions terminated by CH_3; in (a), regions terminated by COOH were <0.5 nm higher than regions terminated by CH_3.

(22) Grafstrom, S.; Nietzert, M.; Hagen, T.; Ackermann, J.; Neumann, R.; Probst, O.; Worge, M. *Nanotechnology* **1993**, *4*, 143–151.

(23) The observation that LFM shows greater contrast between regions of different chemical functionality in patterned SAMs than does NFM is in agreement with previous observations on other substrates. For example, see refs 12, 13, 20, and 21.

(24) DiMilla, P. A.; Folkers, J. P.; Biebuyck, H. A.; Härter, R.; López, G. P.; Whitesides, G. M. *J. Am. Chem. Soc.* **1994**, *116*, 2225–2226.

contrast obtained by LFM (Figure 3b). The increased contrast in these samples was not due to changes in the operation of the NFM. Rather, the increased contrast in these samples was probably due to adsorbates on the (more hydrophilic) COOH regions: for the sample in Figure 3b, regions terminated by COOH were ~2 nm higher than regions terminated by CH_3 (compared to ~0.5 nm in Figure 3a).

The morphology of the substrate did not influence significantly the contrast between regions terminated by CH_3 or COOH. The thickness (and accompanying roughness of the surface) of gold films influences the hysteresis in wetting, conductivity, and opacity of the substrate.[24] Gold substrates typically used in our laboratory have a thickness between 50 and 3000 Å and are prepared by evaporation (by electron-beam heating) of gold onto silicon wafers at room temperature. The gold in the resulting films is polycrystalline, and the domain size and surface roughness increase with the thickness of the gold film. We wanted to determine the role of surface morphology in LFM imaging of patterned SAMs since changes in the curvature of the surface might affect interpretation of changes in contrast between regions of patterned SAMs. A substrate was prepared with two thicknesses of gold (3000 and 300 Å) meeting in a line; the regions of different thickness had different surface morphologies by NFM (Figure 4a). Microcontact printing of this substrate with hexadecanethiol ($HS(CH_2)_{15}CH_3$, darker in Figure 4b), followed by washing with mercaptohexadecanoic acid ($HS(CH_2)_{15}COOH$, brighter in Figure 4b), formed a patterned SAM that extended across areas of both thicknesses. Imaging this patterned SAM by LFM showed similar contrast between CH_3 and COOH groups on areas of the substrate with different morphologies (Figure 4b). We conclude that the morphology of the substrate does not influence significantly the contrast for LFM images of patterned SAMs on gold (at least on gold up to 3000 Å thick).

The elastomeric stamp (used in μCP) evidently conformed well to the surface along the border between regions with different thicknesses of gold: contrast for regions of the SAMs formed by μCP (darker in Figure 4b) was largely uninterrupted by this border. SAMs terminated by CH_3 formed in areas that did not correspond to the pattern of the stamp (white arrow, Figure 4b). This aberration in the μCP process occurred only along the border between regions with different thicknesses of gold. We did not investigate the mechanism for this process, but we speculate that it occurs by reactive spreading ("wicking") of hexadecanethiol along the groove formed by the step between the two regions of gold of different thicknesses.

Contrast between regions of patterned SAMs terminated by CH_3 and COOH was not influenced by the relative humidity of the atmosphere surrounding the sample. We prefer to image substrates by LFM under ambient laboratory conditions rather than in a controlled atmosphere because it is more convenient. We wanted to test whether changes in humidity (and therefore changes in the thickness in films of water adsorbed on the substrate) affected contrast between regions of patterned SAMs imaged by LFM. Patterned SAM with regions terminated by CH_3 or COOH gave similar contrast in air (relative humidity ~40–60%) or dry nitrogen by LFM (Figure 5a,b).

We also used force modulation microscopy (FMM) to image patterned SAMs and to test whether changes in the humidity of the imaging environment affected contrast. FMM measures the force exerted on the AFM cantilever by the surface of the sample with changes in the distance between the sample and the fixed end of the cantilever (Figure 6a,b). In a typical FMM measurement: (i) the

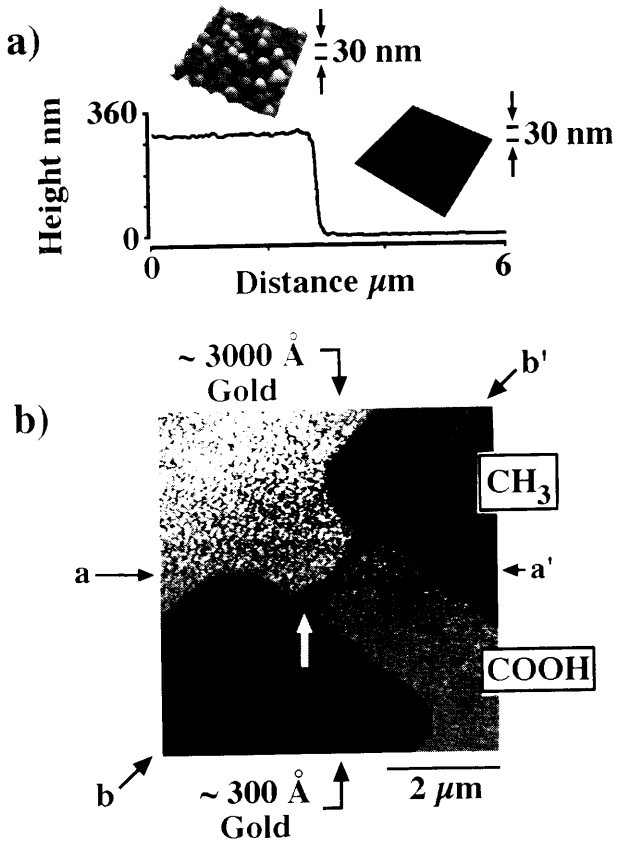

Figure 4. (a) Evaporation of gold on silicon wafers patterned by optical lithography (see Experimental Section) resulted in a sample with adjacent regions of gold with different thicknesses. Crystallites of gold on each half of the sample had a size and distribution characteristic of the thickness of the gold as measured by NFM (insets, a). The two insets have the same vertical scale (0–30 nm) and horizontal dimensions of 1 μm. (b) Observation of contrast by LFM between adjacent regions in patterned SAMs with terminal CH_3 groups (dark) or terminal COOH groups (light) on 3000 Å thick gold was similar to contrast between these groups on 300 Å thick gold. The pattern in CH_3 groups was formed first by microcontact printing; the region terminated by COOH was formed second. The horizontal arrows a and a′ in (b) mark the endpoints of a line shown as a topological profile in (a). The arrows b and b′ mark the endpoints of the line tracing the border between regions of different thicknesses of gold. The white arrow denotes a region of SAM terminated by CH_3 groups (the groups printed in the μCP step) that formed even though the elastomeric stamp did not come into contact with this region of the surface. See text for details.

scan stopped; (ii) the sample moved 10 nm away from its feedback point, and out of contact with the tip (Figure 6c, A); (iii) the sample (out of contact) moved toward the tip (Figure 6c, A–B): the cantilever experienced no force in this regime; (iv) contact between the sample and tip was established (Figure 6c, B–C); (v) the sample continued to move into (and press against) the tip causing the cantilever to bend. This bending changed the position of the light on the photodetector: Positive change in the difference signal between top and bottom halves of the photodetector corresponded to increasing force exerted on the tip (and cantilever) by the surface (Figure 6c, C–D). The average slope (dF/dZ) of the line C–D was measured at each point on the substrate. A plot of the average slopes at each point on the substrate was the FMM image (Figure 5c,d). Higher slopes (larger dF/dZ) appeared in the image as brighter pixels; lower slopes (smaller dF/dZ) appeared as darker pixels.

Imaging a patterned SAM by FMM under ambient conditions produced contrast between regions of a patterned SAM terminated by CH_3 and COOH (Figure 5c). As with the LFM images, brighter regions (in Figure 5c,d)

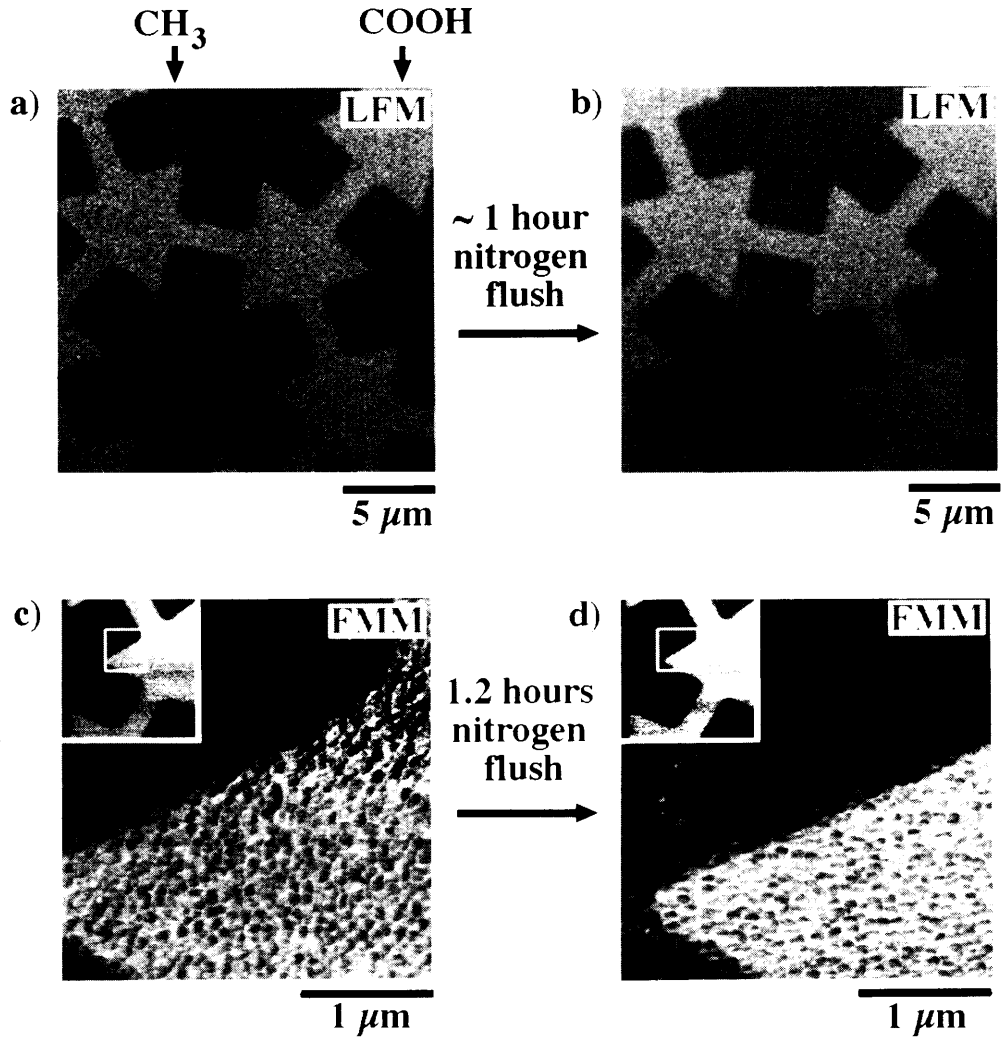

Figure 5. LFM and force modulation microscopy (FMM) detected changes in chemical functionality in adjacent regions of patterned SAMs terminated by CH_3 or COOH. (a) LFM imaging of the patterned SAM in an inert environment (dry N_2) did not alter significantly the contrast between adjacent regions terminated by CH_3 or COOH compared to imaging of these samples in air (b). (c) Imaging patterned SAMs by FMM in an inert environment (dry N_2) also did not alter significantly the contrast between adjacent regions terminated by CH_3 or COOH compared to imaging of these samples in air (d). The insets (c, d) show images (by LFM) of the larger areas (50 μm^2) that encompassed the detailed regions (white boxes in the insets) imaged by FMM.

corresponded to areas of the surface with SAMs terminated by COOH; darker regions corresponded to areas with SAMs terminated by CH_3. A bright region corresponds to a larger slope than a dark region: that is, a surface terminated by COOH is "stiffer" than a surface terminated by CH_3. Imaging the same sample by FMM in an inert environment of N_2 did not alter significantly this contrast (Figure 5d). FMM provides a useful complement to LFM imaging, although acquiring an image required significantly longer times in our experiments (4×) because the tip was pulled out of feedback at each point in the image.

Chemical functionality dominates contrast in images of patterned SAMs by LFM. Patterned self-assembled films terminated by CH_3, OH, and COOH, and mixtures of these groups (see below), provided a useful test of the sensitivity of LFM to the different functionalities that also control interfacial properties of SAMs. Imaging by LFM showed contrast between regions terminated by CH_3, OH, or COOH (Figure 7a,b).

The patterned SAMs in Figure 7a-b resulted from two μCP steps. Microcontact printing 11-hydroxyundecanethiol on gold gave a series of broad parallel lines (of a SAM terminated by OH) with a width of 5 μm. Another series of lines of SAM, orthogonal to the first lines and terminated by COOH, resulted from μCP with mercaptohexadecanoic acid. Rinsing the SAM with a 5 mM ethanolic solution of hexadecanethiol completed the SAM in regions of the gold surface that remained bare. Each μCP step was carried out under water to limit the spread of thiol.[14]

The lateral force measured between the tip and substrate increased with the surface tension (γ_{sv}) of the SAM (CH_3 < OH < COOH),[25] Figure 7c). Deviations from the mean force evident in Figure 7c were smallest for regions terminated by CH_3 and also increased with γ_{sv}. We do not have sufficient experimental data to propose a microscopic interpretation for these deviations. Trends in the deviations from the mean force appeared similar on different samples and under different imaging conditions (see above), so these deviations did not result simply from experimental noise in the acquisition of signal from the tip.

Imaging by LFM revealed the degree of completion of patterned SAMs formed by μCP. Mixing of SAMs terminated by CH_3, OH, or COOH could occur if the μCP process formed incomplete monolayers: subsequent stamping or washing of the surface (using alkanethiols terminated by functional groups differing from the initial stamping) would derivatize those regions of the surface without a complete monolayer. In most cases, we observed homogeneous contrast in regions of SAMs terminated by different chemical functionalities (CH_3, OH, and COOH,

(25) Chaudhury, M. K.; Whitesides, G. M. *Science* **1992**, *255*, 1230–1232.

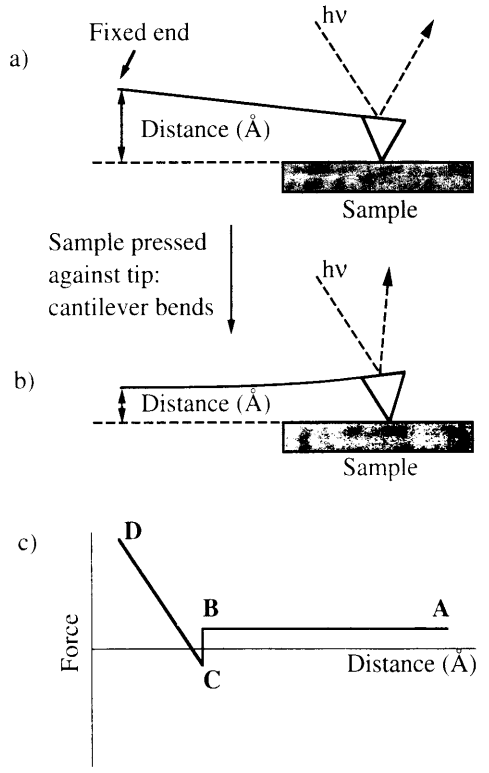

Figure 6. Schematic of force modulation microscopy (FMM) measurements and the resulting force–distance curves. (a–b) Changing the distance between the sample and the fixed end of the AFM cantilever exerted force on this cantilever, causing it to bend. This bending changed the position of the light (reflected off the cantilever) on a photodetector. (c) The force exerted on the tip (and cantilever) by the sample changed with the distance between the sample and the fixed end of the cantilever.

Figure 7a,b). These regions had sharp boundaries (<250 nm) and showed no evidence of mixing of different chemical functionalities (by visual inspection of the contrast).

Transfer of incomplete SAMs to specific regions of the gold by μCP, creating SAMs with mixtures of functional groups (CH_3, OH, and COOH) at the SAM/air interface was also possible. Repeated stamping on gold without reapplication of thiol to the PDMS stamp partially depleted the amount of alkanethiol in the stamp; μCP with this "depleted" stamp on the substrate of interest thus transferred only enough thiol to the gold surface to form an incomplete ("depleted") SAM.

The patterned SAMs in Figure 7d resulted from μCP with "depleted" PDMS stamps (see above). Microcontact printing 11-hydroxyundecanethiol on gold (with a depleted PDMS stamp) gave parallel lines of partial SAMs terminated by OH; the gold surface was not covered completely by the OH-terminated monolayer. Another series of lines (of partial SAMs), terminated by COOH and orthogonal to (and intersecting) the first lines, resulted from μCP mercaptohexadecanoic acid with a "depleted" stamp. This μCP step also created mixed SAMs terminated by OH and COOH where the stamp delivered mercaptohexadecanoic acid to regions of the gold surface covered partially with SAMs terminated by OH (from the first μCP step). Rinsing the substrate with a 5 mM ethanolic solution of hexadecanethiol formed complete SAMs terminated by CH_3 in regions of the gold surface that remained bare and completed the SAMs (forming mixed SAMs) in those regions where μCP had formed only partial SAMs.

LFM was sensitive to regions in SAMs where mixtures of functional groups (CH_3, OH, and COOH) were present (Figure 7d). Previous images (Figure 7a,b) established

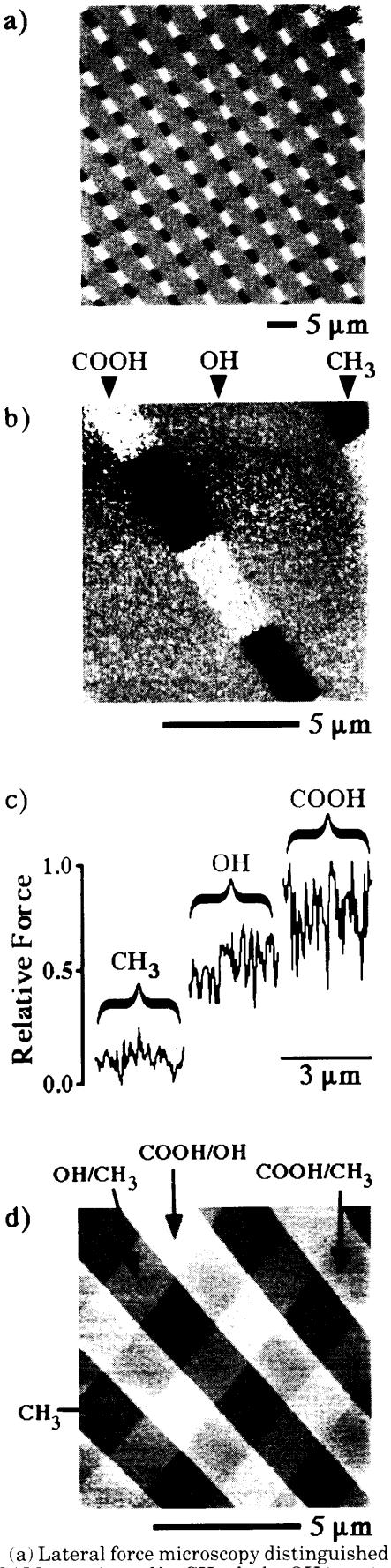

Figure 7. (a) Lateral force microscopy distinguished between regions of SAMs terminated by CH_3 (dark), OH (gray), or COOH (light) and mixtures of these functional groups. (b) No evidence of mixing between regions of patterned SAMs terminated by different functional groups was evident by visual inspection of the contrast. (c) The relative lateral force between the tip and the surface, and the fluctuations in this force, increased with an increase in the surface-free energy of the SAM. (d) LFM imaged SAMs with mixtures of different terminal groups (see text for details).

the relative contrast between regions of unmixed SAMs terminated by different chemical functionalities: CH_3 < OH < COOH. We assumed that the brightness of the pixels (in the LFM image) for patterned SAMs terminated by a mixture of two functional groups was intermediate between the brightness of the pixels for unmixed SAMs terminated by the constituent alkanethiols of the mixture (e.g. CH_3 < CH_3/OH < OH). We thus identified regions of different contrast observed in Figure 7d: (i) the darkest regions in Figure 7d corresponded to regions of SAMs terminated only by CH_3; (ii) the brightest regions in Figure 7d corresponded to regions with a mixture of SAMs terminated by OH/COOH (there are no regions corresponding to SAMs terminated only by COOH or OH); (iii) regions of the patterned SAM with intermediate brightness were assigned CH_3/OH < CH_3/COOH. We cannot rule out the possibility that the brightest regions in the image correspond to a tertiary mixture of SAMs terminated by mixtures of OH/COOH/CH_3.

The ability to form and image (by LFM) SAMs with regions terminated by mixtures of different chemical functionalities may find use in the fabrication of surfaces with well-defined gradients in their interfacial properties in μm^2 regions.

Conclusions

This paper demonstrates that scanning probe microscopies (LFM, NFM, and FMM) can provide excellent imaging of patterned SAM formed by microcontact printing. LFM and FMM showed contrast between regions of patterned SAMs terminated by different chemical functionalities. NFM typically showed less contrast than LFM or FMM but provided topographical information. Chemical functionality dominated the imaging process in these experiments; the morphology of the underlying surface and the humidity of the environment for imaging did not influence the contrast in our experiments.

The use of LFM in imaging patterned SAMs provides high contrast and convenience. It also opens a window into tribology on the 100-nm scale. Although we have not yet explored this area quantitatively, the structural flexibility of SAMs, which provides the ability to present a wide range of well-defined functional groups at a surface, makes this system attractive for correlating microscopic and macroscopic studies of tribology.

Experimental Section

Instrumentation. Scanning probe microscopy measurements (NFM, LFM, FMM) were performed with a Topometrix TMX 2010 scanning probe microscope (Mountain View, CA). A cantilever fabricated from silicon nitride, in constant contact with the surface, scanned across the substrate at a constant rate (~1–150 μm/s, depending on the size of the region being scanned) and with a constant force (~0.1 nN). We obtained simultaneously LFM images and NFM images. FMM images were obtained simultaneously with NFM images.

Materials. Absolute ethanol (Quantum Chemical Corp.) was bubbled with dry N_2 (to remove oxygen) prior to use. Hexadecanethiol (Aldrich) was purified by column chromatography prior to use. All other thiols were available from previous studies or were synthesized according to literature preparations.[26]

Substrate Preparation. Electron-beam evaporation of gold (Materials Research Corp., Orangeburg, NY; 99.999%) onto silicon [100] test wafers (Silicon Sense, Nashua NH) at room temperature provided 5–3000 Å thick gold films. Titanium (Johnson Mathey, 99.99%; ~5–25 Å thick) was an adhesion promoter between the gold and silicon oxide.

We prepared substrates with adjacent regions of gold of different thickness by standard photolithographic techniques (Figure 8). Spin-coating deposited photoresist (Shipley, Marlborough, MA, Microposit 1813) on a silicon [100] wafer (Figure 8a). We exposed this wafer to UV light though a mask of parallel lines; developing the exposed areas of the photoresist formed a pattern with lines of photoresist (and spaces of bare silicon oxide) on this wafer (Figure 8b). Electron-beam evaporation deposited a ~2700 Å thick gold film on the substrate (10 Å of titanium was used as the adhesion promoter). Gold films residing on the photoresist pattern were selectively removed by lifting the photoresist (and the gold adhered to the photoresist) from the wafer; this "liftoff" process was accomplished by soaking the substrate in acetone for ~30 min, with occasional (two to four) short (<5 s) bursts of sonication. The sample was repeatedly washed with acetone, water, heptane, and ethanol, and dried under a stream of N_2 gas. This process did not remove gold attached to the bare silicon oxide (Figure 8c). A ~300 Å gold film (with 5 Å of Ti as an adhesion promoter) was then deposited on the entire surface of the sample by electron beam evaporation at 1 Å/s (Figure 8d).

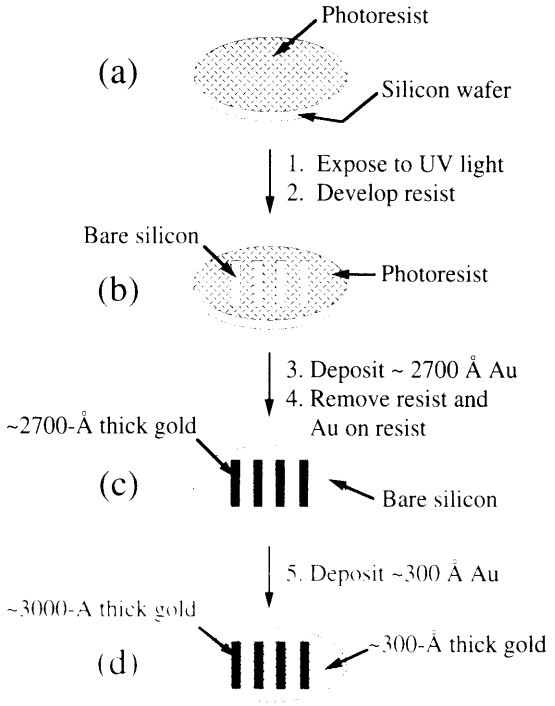

Figure 8. Photolithography and deposition of gold (by electron-beam evaporation) prepared a substrate with two thicknesses of gold (3000 and 300 Å) meeting in a line. (a) Spin-coating deposited photoresist on a silicon wafer. (b) Exposure to UV light (through a mask of lines) and developing removed photoresist in a pattern corresponding to the lines of the photomask. (c) Electron-beam evaporation of gold deposited a ~2700 Å thick gold surface on the substrate. Exposure to acetone removed the photoresist (and with it the gold on the photoresist); gold on regions not covered by photoresist remained on the substrate. (d) Electron-beam evaporation of gold deposited a ~300 Å thick layer of gold on the substrate.

Formation of Monolayers. Silicon wafers coated with gold were fractured into rectangular slides (1–2 cm × 4–5 cm), washed with heptane, deionized water, and absolute ethanol, and dried with a stream of dry N_2 gas. Microcontact printing[2,3] (μCP) of alkanethiols using an elastomeric stamp formed patterned SAMs. Patterned SAMs exposed to open air for many days were washed with absolute ethanol, deionized water, and 0.1 N HCl and dried in a stream of dry N_2 before imaging.

Acknowledgment. This work was supported in part by the Advanced Research Projects Agency and the Office of Naval Research. J.L.W. gratefully acknowledges a postdoctoral fellowship from the National Institutes of Health (Grant Number 1-F32 GM16511-01). J.C.M. gratefully acknowledges a postdoctoral fellowship from Merck.

LA9405556

(26) Bain, C. D.; Evall, J.; Whitesides, G. M. *J. Am. Chem. Soc.* **1989**, *111*, 7155–7164.